

Solution Growth and Characterization of 4-Carboxyanilinium Tartrate Single Crystal

C. Muthuselvi, S. Abirami and V. Shanmuga Priya

Department of Physics, Devanga Arts College, Aruppukottai 626101, Tamilnadu, India

ABSTRACT

Background and Objective: The organic compound of 4-carboxyaniline has UV absorption and antifibrotic properties. It was naturally found in *Streptomyces griseus*, *Synechococcus elongatus* and other organisms. In this study, an effort was made to the growth of the 4-carboxyaniline derivative crystal with tartaric acid using the solution growth technique. **Materials and Methods:** The 4-carboxyanilinium tartrate crystal was grown from a slow evaporation technique in an aqueous ethanol solution at room temperature. The grown crystal was characterized by single crystal XRD, powder XRD, FT-IR, FT-Raman, UV-visible spectroscopy, SEM with EDX and antibacterial activity studies. **Result:** The monoclinic crystal system and $P2_1$ space group was confirmed from the single crystal XRD study. The diffraction peaks were indexed using INDX software. The average crystalline size was determined as 55 nm. All the wavenumber assignments were exactly matched with recently reported corresponding compounds. From the optical absorbance data, the band gap was determined as 3.75 eV using Tauc's plot. The well-defined shape of the crystal was confirmed by the SEM micrographs. *Bacillus subtilis* and *Acinetobacter baumannii* exhibited the highest zone of inhibition towards the grown crystal than *Escherichia coli*. **Conclusion:** The finding result of this study supports the previous knowledge of the structural and biological assortment of 4-carboxyanilinium tartrate complex crystals.

KEYWORDS

PABA, vitamin B-complex, optical study, 4-carboxyanilinium, tartrate complex

Copyright © 2022 C. Muthuselvi et al. This is an open-access article distributed under the Creative Commons Attribution License, which permits unrestricted use, distribution and reproduction in any medium, provided the original work is properly cited.

INTRODUCTION

The 4-carboxyaniline also known as 4-aminobenzoic acid or p-ABA, in which the amino and carboxylic acid groups are attached to the benzene ring in para-position^{1,2}. It is a vitamin-like substance, particularly vitamin B-complex and is considered a non-essential nutrient in humans³. The 4-carboxyaniline is used in the synthesis of the vitamin folic acid and is found in several foods including eggs, grains, meat and milk^{4,5}. It is also used to darken grey hair, prevent hair loss, make skin look younger and prevent sunburn and therefore known as an ultraviolet sun screen that is applied to the skin as sun lotions⁶. It is widely used as a therapeutic agent such as an antioxidant, antibacterial, antimutagenic, anticoagulant and fibrinolytic^{7,8}. The 4-carboxyaniline is considered a protective drug against UV-irradiation which could donate and also accept hydrogen through both the amine and carboxylic acid functional groups⁹. The complexes of 4-carboxyaniline had already been studied by many authors to understand their structure extension properties through their hydrogen bonding associations¹⁰⁻¹⁵. The crystal structure of 4-carboxyanilinium



tartrate has already been reported by Athimoolam *et al.*¹⁶. Keeping in view, the structural and biological assortment of the 4-carboxyaniline compound, here report the growth by a slow evaporation method, single crystal XRD, PXRD, FT-IR, FT-Raman, UV-Visible-NIR spectroscopy, SEM with EDX and antibacterial activity studies.

MATERIALS AND METHODS

Study area: The title crystal was developed at the Research Department of Physics, Devanga Arts College, Aruppukottai, Tamilnadu, India in November, 2021. The data were composed between December, 2021 and February, 2022.

Crystal growth: The growing preliminary materials for 4-carboxyanilinium tartrate single crystal were 4-carboxyaniline, tartaric acid and ethanol which were purchased from the Modern Scientific Company, a Laboratory equipment supplier in Madurai, Tamil Nadu. According to the slow evaporation method, a single crystal of 4-carboxyanilinium tartrate was obtained. First, 1.37 g of 4-carboxyaniline was dissolved in the aqueous ethanol solution (50 mL water+50 mL ethanol) and 1.5 g of tartaric acid was dissolved in water with a molar ratio of 1:1. Then these solutions were mixed and stirred well for 1 hr at room temperature. The mixed solutions were poured into the petri dish after filtration. Finally, the title crystals were grown within 10 days. The quality crystals were collected and kept in the zip lock cover. The photographic view and the chemical structure of 4-carboxyanilinium tartrate are shown in Fig. 1 and 2, respectively.

Experimental details: The single crystal X-ray diffraction was performed using Bruker SMART APEX CCD diffractometer with Mo K α radiation ($\lambda = 0.71073 \text{ \AA}$). The powder XRD analysis was carried out by XPERT-PRO X-ray diffractometer with Cu K α radiation (1.54060 \AA) in the 2θ range 20-80°. Using SHIMADZU FT-IR spectrometer in the wavenumber range 400-4000 cm^{-1} with the KBr disc method, the FT-IR spectrum was obtained. The FT-Raman spectrum was prepared with BRUKER: RFS 27 Raman

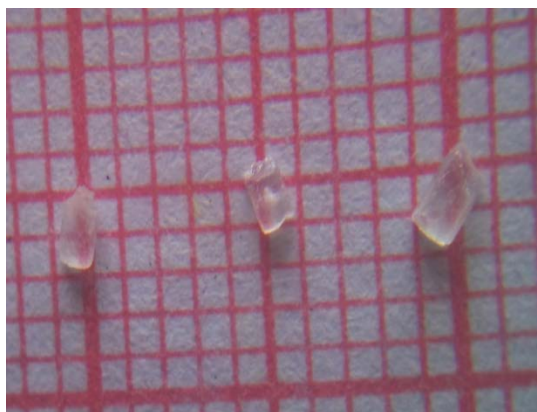


Fig. 1: Grown crystal of 4-carboxyanilinium tartrate

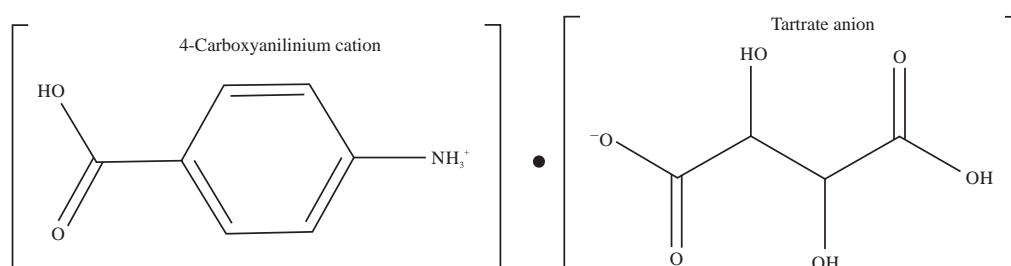


Fig. 2: Chemical structure of 4-carboxyanilinium tartrate crystal

spectrometer in the wavenumber range 4000-400 cm^{-1} . The optical absorbance spectrum had been recorded with SHIMADZU-UV 1601 double beam spectrometer in the wavelength range 190-1100 nm. The SEM with EDX analysis was performed using CARLZEISS EVO18 scanning electron microscope. The antibacterial activity study was performed by agar well diffusion method with the three different microorganisms.

RESULTS AND DISCUSSION

Single crystal XRD analysis: The unit cell dimension was determined as $a = 6.021(4) \text{ \AA}$, $b = 28.789(11) \text{ \AA}$, $c = 7.426(5) \text{ \AA}$, $\alpha = 90^\circ$, $\beta = 107.89(4)^\circ$, $\gamma = 90^\circ$ and volume $V = 1225.0(12) \text{ \AA}^3$ from the single crystal XRD study and other crystallographic data of title crystal is shown in Table 1. The molecular structure of 4-carboxyanilinium tartrate crystal is depicted in Fig. 3. The molecular structure consists of discrete protonated 4-carboxyanilinium cation and deprotonated tartrate anion which are linked together through N-H...O hydrogen bonding to form the molecular complex. The title crystal belongs to the monoclinic crystal system with space group $P2_1$. All the unit cell parameters are exactly matched with the already reported values of the same compound by Athimoolam *et al.*¹⁶.

Table 1: Lattice parameters of 4-carboxyanilinium tartrate crystal

Lattice parameters	Current work	Reported work ¹⁶
Compound names	4-Carboxyanilinium tartrate	4-Carboxyanilinium tartrate
Empirical formula	$\text{C}_7\text{H}_8\text{NO}_2^+ \cdot \text{C}_4\text{H}_5\text{O}_6^-$	$\text{C}_7\text{H}_8\text{NO}_2^+ \cdot \text{C}_4\text{H}_5\text{O}_6^-$
Molecular weight	287.22	287.22
Crystal system	Monoclinic	Monoclinic
Space group	$P2_1$	$P2_1$
Unit cell dimensions	$a = 6.025(6) \text{ \AA}$ $b = 28.790(12) \text{ \AA}$ $c = 7.430(7) \text{ \AA}$ $\alpha = 90^\circ$ $\beta = 107.92(5)^\circ$ $\gamma = 90^\circ$	$a = 6.021(4) \text{ \AA}$ $b = 28.789(11) \text{ \AA}$ $c = 7.426(5) \text{ \AA}$ $\alpha = 90^\circ$ $\beta = 107.89(4)^\circ$ $\gamma = 90^\circ$
Volume	$1227.0(14) \text{ \AA}^3$	$1225.0(12) \text{ \AA}^3$

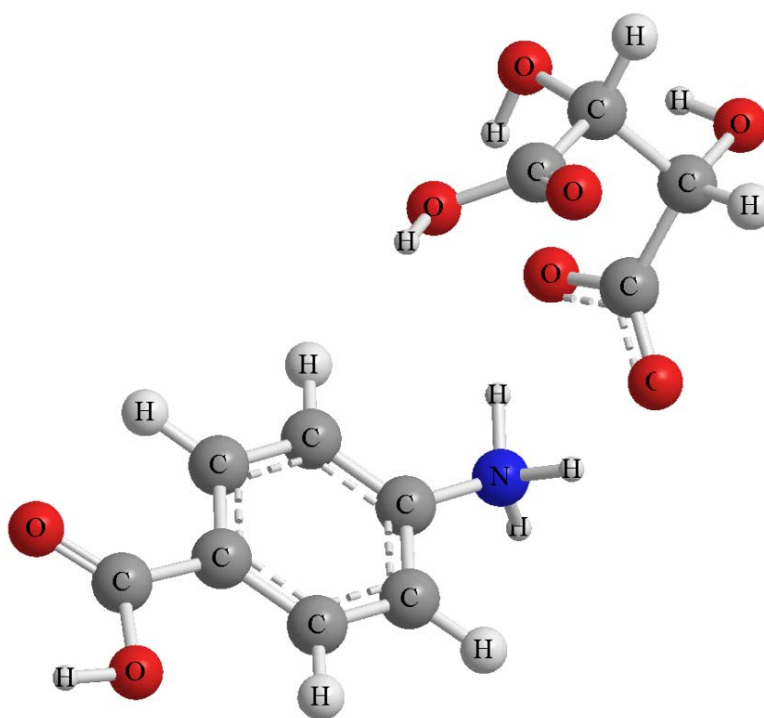


Fig. 3: Molecular structure of 4-carboxyanilinium tartrate crystal

Determination of crystalline size: The 4-carboxyanilinium tartrate crystal was finely ground, homogenized and the diffraction pattern was recorded. The experimentally recorded powder diffraction data is shown in Fig. 4. The one-dimensional distribution in diffraction intensities shows that every substance in the grown material produces its diffraction pattern. The highest peak appeared at 24.62°. Indexing of peaks was carried out using INDX software. This PXRD analysis reveals the good crystalline nature of the title crystal. The average crystalline size was determined as 55 nm using the Debye-Scherrer formula and also the dislocation density was calculated as $3.306 \times 10^{14} \text{ m}^{-2}$ using the formula:

$$\delta = \frac{1}{D^2} \text{m}^2$$

FT-IR and FT-Raman spectroscopy analysis: The 4-carboxyanilinium tartrate crystal has a di-substituted benzene ring in the para position, $-\text{[NH}_3\text{]}^+$, $-\text{COOH}$, $-\text{C(OH)}$ and COO^- functional groups. The vibrational IR and Raman spectra are shown in Fig. 5 and 6, respectively. The detailed wavenumber and functional group assignment are given accordingly in Table 2.

Vibrations of 4-carboxyanilinium cation

Para substituted benzene ring: The C = C and C-C ring stretching modes normally appear in the region $1650\text{-}1430 \text{ cm}^{-1}$ and $1400\text{-}1300 \text{ cm}^{-1}$, respectively¹⁷. The $\nu(\text{C}=\text{C})$ mode was attributed at 1607, 1584 and

Table 2: Wavenumber and functional group assignments for 4-carboxyanilinium tartrate crystal in FT-IR and FT-Raman spectra

FT-IR ($\bar{\nu} \text{ cm}^{-1}$)	FT-Raman ($\bar{\nu} \text{ cm}^{-1}$)	Assignment
3422 (s, br)	-	$\nu_{\text{as}}(\text{O-H})_{\text{water}}$
3406 (s, br)	-	$\nu_{\text{as}}(\text{O-H})_{\text{water}}$
3321 (sh)	-	$\nu_{\text{s}}(\text{O-H})_{\text{water}}$
3265 (m)	-	$\nu_{\text{s}}(\text{O-H})_{\text{water}}$
3179 (m)	-	$\nu_{\text{as}}[-\text{NH}_3]^+$
3150 (m)	-	$\nu_{\text{as}}[-\text{NH}_3]^+$
-	3084 (s)	$\nu(\text{C-H}), \nu(-\text{OH})_{\text{acid}}$
-	3015 (m)	$\nu(\text{C-H}), \nu(-\text{OH})_{\text{acid}}$
2970 (m)	2985 (m)	$\nu_{\text{s}}[-\text{NH}_3]^+, \nu_{\text{as}}(\text{C-H})_{\text{tartrate}}, \nu(-\text{OH})_{\text{acid}}$
2922 (m)	2940 (m)	$\nu_{\text{s}}[-\text{NH}_3]^+, \nu_{\text{s}}(\text{C-H})_{\text{tartrate}}, \nu(-\text{OH})_{\text{acid}}$
1726 (s, br)	1714 (s)	$\nu_{\text{as}}(\text{C=O})_{\text{acid}}$
1636 (m)	-	$\nu_{\text{s}}(\text{C=O})_{\text{acid}}, \beta(\text{O-H})_{\text{water}}$
1607 (m)	1615 (s)	$\nu(\text{C=C})$
1584 (m)	-	$\nu(\text{C=C}), \nu_{\text{as}}(\text{COO}^-), \rho[-\text{NH}_3]^+$
1510 (m)	-	$\nu(\text{C=C})$
1422 (m)	-	$\nu_{\text{as}}(\text{COO}^-), \beta(-\text{OH})_{\text{acid}}$
1337 (m)	1337 (m)	$\nu_{\text{s}}(\text{COO}^-), \nu(\text{C-C}), \beta(-\text{OH})_{\text{acid}}$
1308 (s)	-	$\nu(\text{C-N}), \beta(\text{C-H})_{\text{tartrate}}, \nu(\text{C-C}), \nu(\text{C-O})$
1240 (s)	1252 (w)	$\nu(\text{C-O})$
-	1210 (m)	$\nu(\text{C-O})$
1177 (m)	-	$\tau[-\text{NH}_3]^+, \beta(\text{C-H})$
1130 (s)	1136 (m)	$\beta(\text{C-H})$
1099 (m)	1112 (m)	$\beta(\text{C-H})$
1074 (s)	-	$\nu(-\text{OCH})$
1018 (m)	-	$\nu(-\text{OCH})$
986 (m)	-	$\gamma(-\text{OH})_{\text{acid}}$
897 (m)	897 (m)	$\gamma(-\text{OH})_{\text{acid}}$
837 (m)	835 (s)	Benzene ring breathing mode
783 (w)	-	$\gamma(\text{C-H})$
758 (m)	-	$\gamma(\text{C-H})$
729 (w)	-	$\gamma(\text{C-H})$
683 (m)	639 (m)	$\gamma(\text{C-H})_{\text{tartrate}}, \rho(\text{O-C=O}), \rho(\text{COO}^-)$
611 (m)	-	$\omega(\text{COO}^-), \tau(-\text{OH})_{\text{acid}}, \omega(\text{O-C=O}), \gamma(\text{C-H})_{\text{tartrate}}$
600 (m)	-	$\tau[-\text{NH}_3]^+, \tau(\text{O-C=O}),$
548 (m)	-	$\tau(\text{COO}^-), \tau(-\text{OH})_{\text{acid}}$
420 (s)	-	$\tau(-\text{OH})_{\text{acid}}$

s: Strong, m: Medium, w: Weak, sh: Shoulder, u: Stretching, ν_{s} : Symmetric stretching, ν_{as} : Antisymmetric stretching, β -in-plane bending, γ - out-of-plane bending, ρ : Scissoring, ω : Wagging, τ : Rocking and t: Twisting

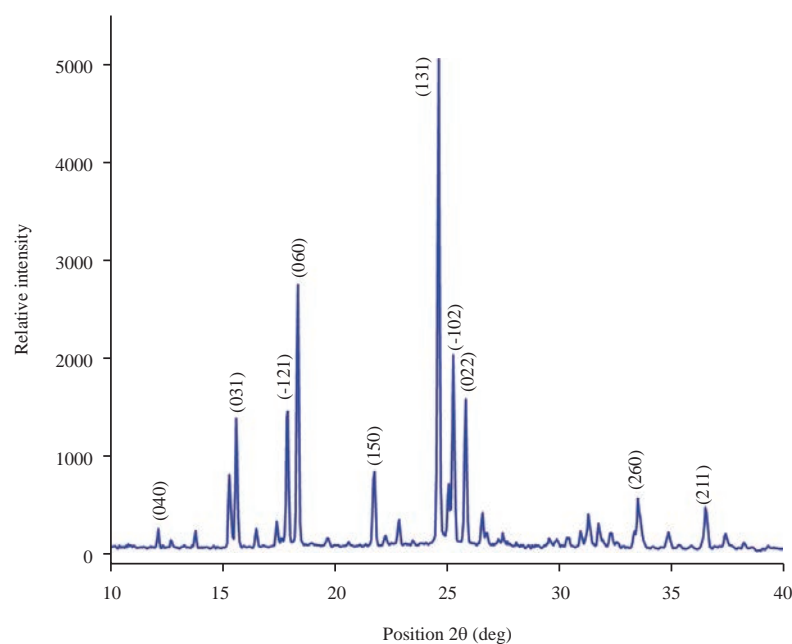


Fig. 4: Diffraction peaks for 4-carboxyanilinium tartrate crystal

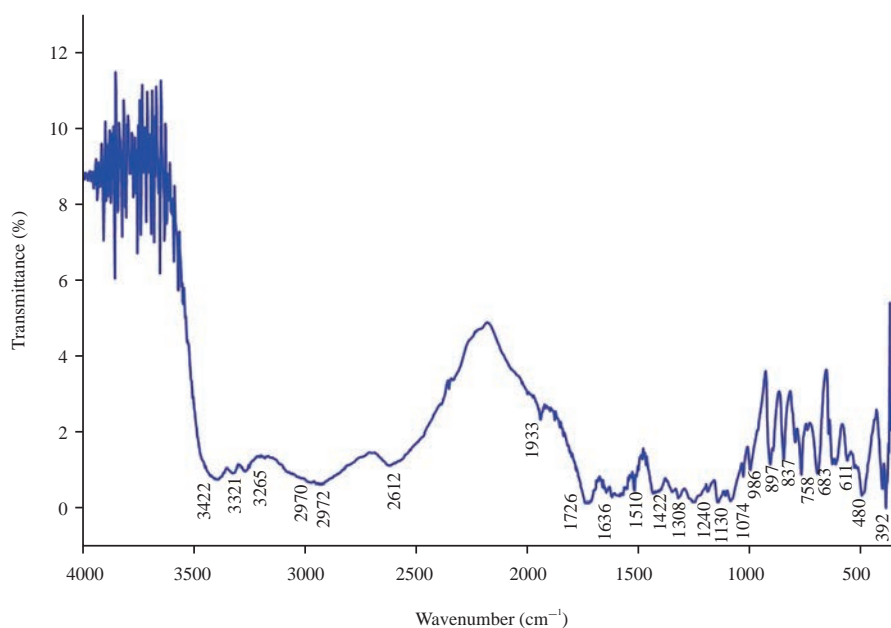


Fig. 5: FT-IR spectrum for 4-carboxyanilinium tartrate crystal

1510 cm^{-1} in infrared and at 1615 cm^{-1} in Raman spectra. Also, ν (C-C) mode was identified at 1337 cm^{-1} and 1308 cm^{-1} in the IR spectrum. Also, the C-N stretching mode was identified at 1308 cm^{-1} . The ring breathing mode was identified at 837 cm^{-1} in IR and 835 cm^{-1} in Raman spectra. The C-H stretching mode of the para-substituted benzene ring is expected in the region 3115-3005 cm^{-1} ¹⁸. In the present study, the bands observed at 3084 cm^{-1} and 3015 cm^{-1} in the Raman spectrum were assigned to the ν (C-H) mode. The in- and out-of-plane bending vibrations of C-H appear in the range 1250-1000 and 900-690 cm^{-1} , respectively¹⁸. The in-plane bending mode β (C-H) was identified at 1240, 1177, 1130, 1099 cm^{-1} in FT-IR and at 1252, 1136, 1112 cm^{-1} in FT-Raman spectra, respectively. The out-of-plane bending mode γ (C-H) was pragmatic at 783, 758 and 729 cm^{-1} in the IR spectrum only.

Carboxylic acid group: The bands recorded at 2970, 2922 cm^{-1} in IR and at 3084, 3015, 2985 and 2940 cm^{-1} in Raman spectra were assigned to the O-H stretch from CO-OH group. The in-plane and

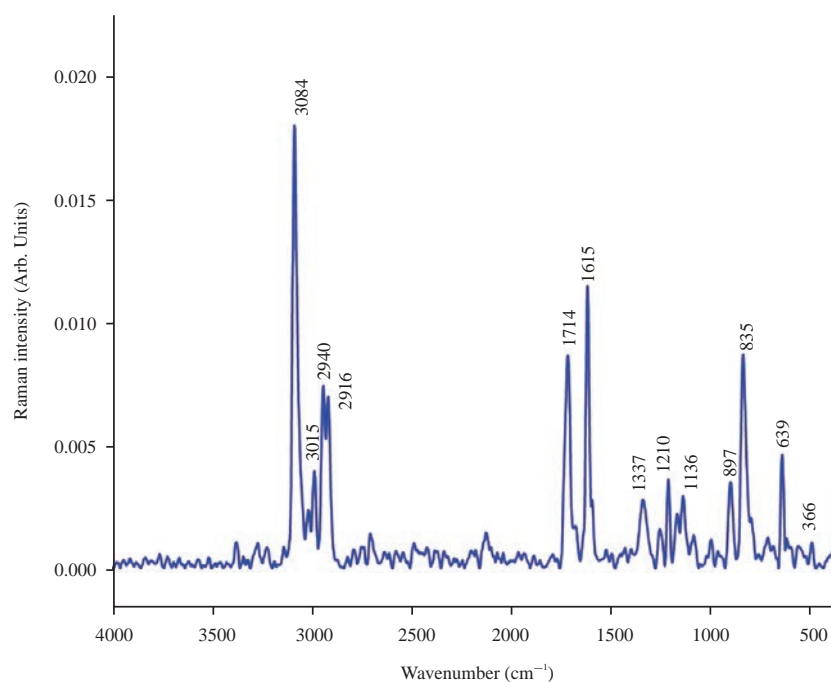


Fig. 6: FT-Raman spectrum for 4-carboxyanilinium tartrate crystal

out-of-plane bending wavenumbers of the O-H group occur between 1440-1395 and 960-875 cm^{-1} , respectively¹⁹. In the present work, β (O-H) and γ (O-H) modes were observed at 1422, 1337 cm^{-1} and 986, 897 cm^{-1} , respectively. The O-H twisting mode was expected to appear at 611, 548, 420 cm^{-1} . The ν_{as} (C = O) mode has the absorbance bands at 1726 and 1714 cm^{-1} in both spectra. Also, bands at 1636 cm^{-1} in IR were assigned to the ν_{s} (C = O) mode. The ν (C-O) mode occurs in the characteristic region of 1320-1210 cm^{-1} ^{17,19}. The title compound has the wavenumbers at 1308, 1240 cm^{-1} in IR and 1252, 1210 cm^{-1} in Raman spectra was attributed to ν (C-O) mode. The scissoring, wagging and rocking modes of the O-C=O group were familiar at 683, 611 and 600 cm^{-1} , respectively.

Anilinium group: For anilinium $-\text{[NH}_3\text{]}^+$ group, the antisymmetric and symmetric stretching mode is normally identified in the region of 3200 and 2800 cm^{-1} ^{19,20}. For the title compound, the bands attributed at 3179, 3150 cm^{-1} for $\nu_{\text{as}}-\text{[NH}_3\text{]}^+$ mode. Also, $\nu_{\text{s}}-\text{[NH}_3\text{]}^+$ mode was observed at 2970, 2922 cm^{-1} in IR and 2985, 2940 cm^{-1} in Raman spectra. The scissoring, rocking and twisting modes of the $-\text{[NH}_3\text{]}^+$ group were identified at 1584, 1177 and 600 cm^{-1} in the IR spectrum, respectively.

Vibrations of tartrate anion: The antisymmetric and symmetric stretching modes of the C-H group were attributed at 2970 and 2922 cm^{-1} . The C-H out-of-plane bending vibration was identified at 683 cm^{-1} and 611 cm^{-1} in the IR spectrum. The C-H in-plane bending mode was observed at 1308 cm^{-1} in the IR spectrum. The stretching -OCH mode of tartrate is seen in the range 1068 cm^{-1} ²¹. The peak that appeared at 1074 and 1018 cm^{-1} in the FT-IR spectrum was assigned to the ν (-OCH) mode for the title crystal. The vibration band was identified at 1584 cm^{-1} in IR for the antisymmetric mode of the COO^- group. Also, the symmetric stretching mode for the same group was identified at 1337 cm^{-1} in both spectra. The scissoring, wagging and rocking deformation modes were recorded at 683, 611 and 548 cm^{-1} , respectively. All these wavenumber assignments are exactly in concurrence with the recently reported values of related compounds²². The wavenumber assignments for carboxylic group vibrations present in tartrate anion are seen in Table 2.

Vibrations of the water molecule: Water was trapped between the Kbr particles during pellet preparation and so the additional peaks were observed in the FT-IR spectrum. The water molecule has two

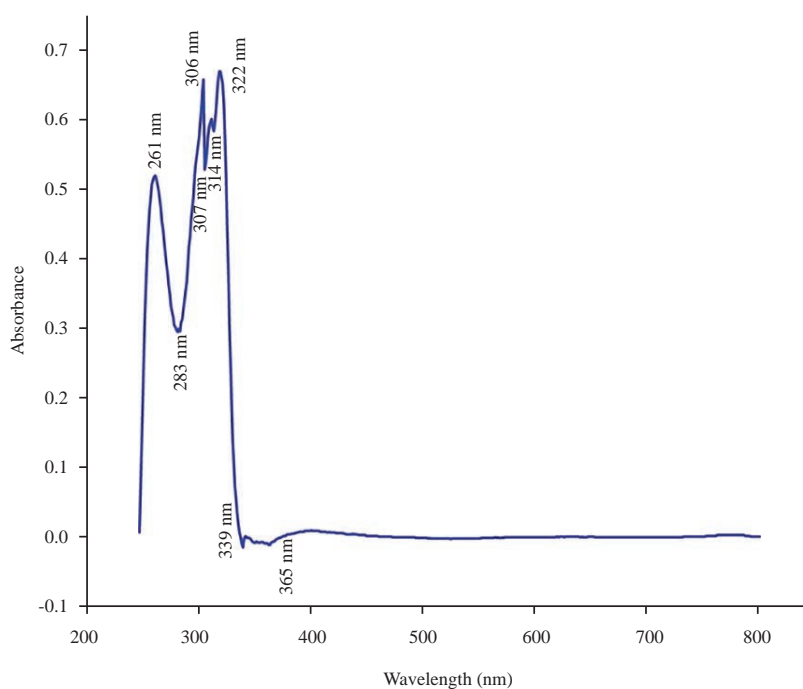


Fig. 7: Optical absorbance spectrum for 4-carboxyanilinium tartrate crystal

Table 3: Composition of (%) elements in 4-carboxyanilinium tartrate crystal

Elements	Weight (%)	Atomic (%)	Error (%)	K ratio
C	43.0	49.8	5.7	0.2558
N	6.2	6.2	16.8	0.0080
O	50.8	44.1	9.7	0.1002

OH stretching modes around 3600 cm^{-1} and one bending mode around 1630 cm^{-1} ²⁰. Strong infrared bands located at 3422 , 3406 and 3321 , 3265 cm^{-1} were attributed, respectively, to the antisymmetric and symmetric stretching vibration of a water molecule. A medium infrared band at 1636 cm^{-1} was assigned to the in-plane deformation mode of a water molecule.

Optical absorbance spectroscopy analysis: The recorded optical absorbance spectrum of 4-carboxyanilinium tartrate crystal is shown in Fig. 7. The crystal absorbs maximum ultraviolet radiation in the wavelength of 261, 306 and 322 nm. The lower cut-off wavelength was found to be at 283, 307, 314, 339 and 365 nm. The title crystal has 100% transmittance in the entire visible region. The optical band gap E_g is determined using Tauc's relation $(\alpha h\nu)^2 = A(h\nu - E_g)$. The calculations were performed using origin software. Then the Tauc plot was drawn by plotting the $(\alpha h\nu)^2$ Vs photon energy and extrapolating the linear portion of $(\alpha h\nu)^2$ to the photon energy axis directly giving the optical band gap value. From Fig. 8, the optical band gap was determined as 3.75 eV for a 4-carboxyanilinium tartrate crystal.

Scanning electron microscopy (SEM) with energy dispersive X-ray spectroscopy (EDX) analysis: SEM/EDX study was used to analyze the surface morphology as well as the presence of elements in a 4-carboxyanilinium tartrate single crystal. The captured SEM micrographs are shown in Fig. 9a and b with 500x and 2.5kx magnifications. The SEM micrographs revealed that the grown crystal has a well-defined shape throughout the surface. The recorded EDX pattern is shown in Fig. 10 which reveals that the carbon atom has the highest counts than the oxygen and nitrogen compounds. The C, N and O elements have the atomic percentage of 49.8, 6.2 and 44.1%, respectively. The element, weight (%), atomic (%), error (%) and K ratio of all the elements present in the 4-carboxyanilinium tartrate crystal are presented in Table 3. The EDX study confirms that tartaric acid was incorporated with the 4-carboxyaniline compound.

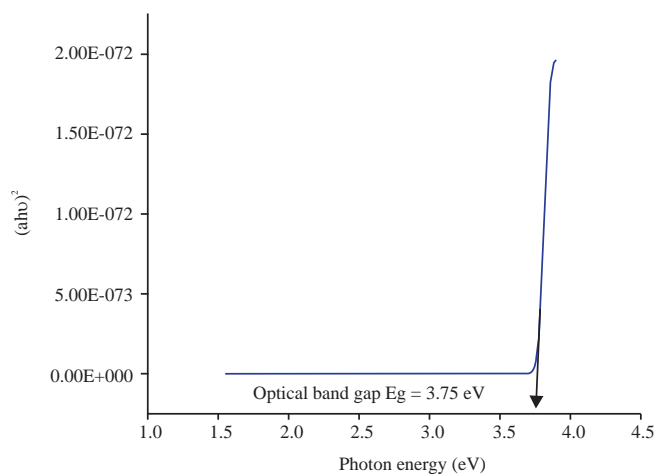


Fig. 8: Tauc plot for 4-carboxyanilinium tartrate crystal

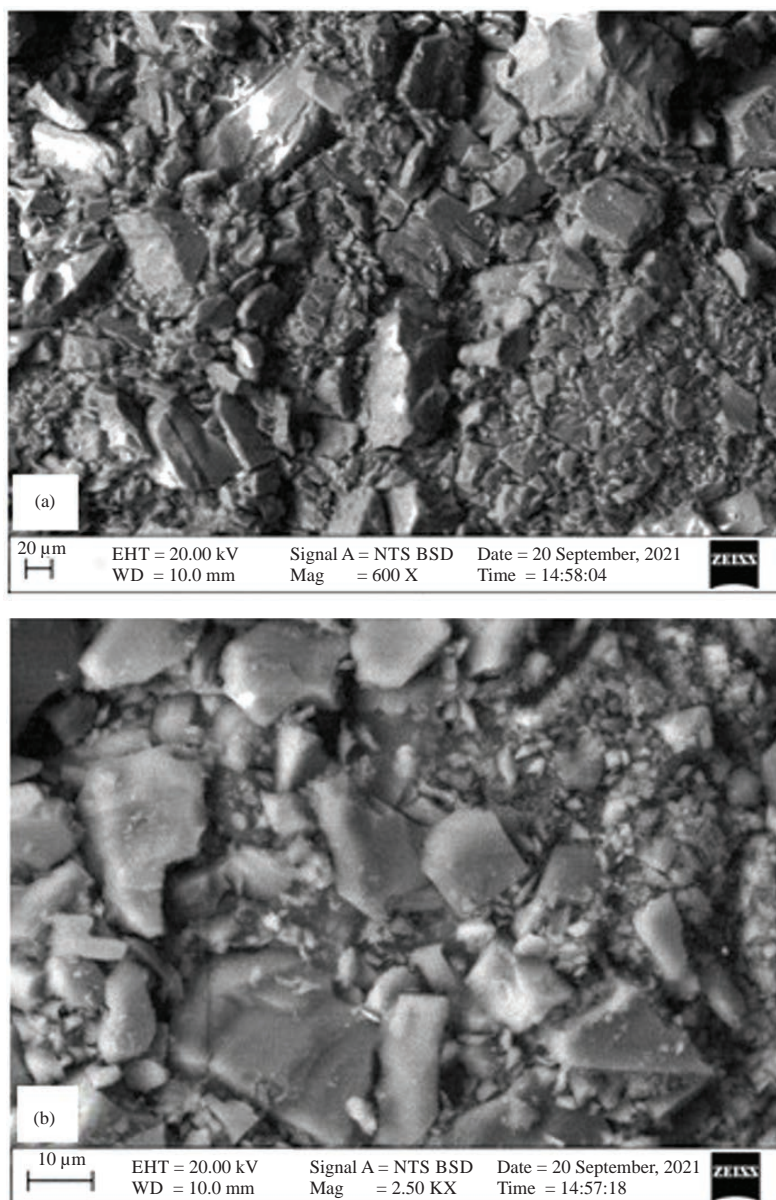


Fig. 9(a-b): SEM micrographs of 4-carboxyanilinium tartrate crystal, (a) 500X magnification and (b) 2.5 kX magnification

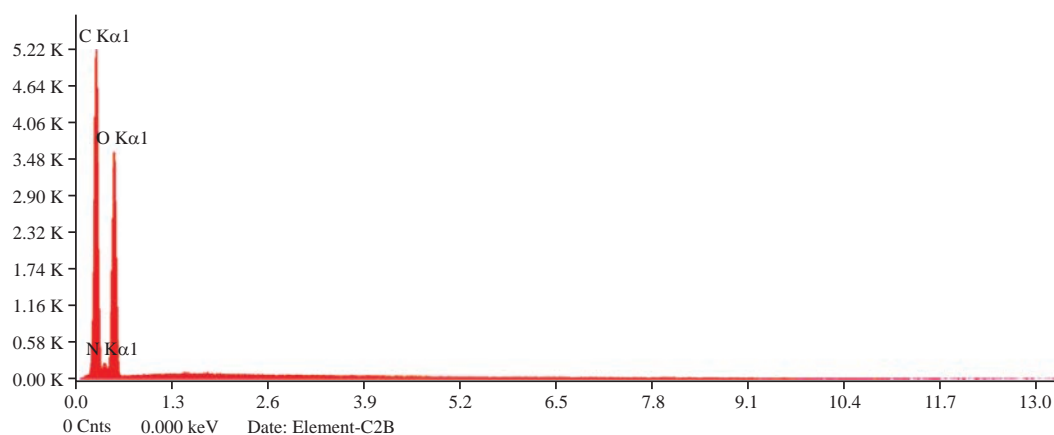


Fig. 10: EDX spectrum of 4-carboxyanilinium tartrate crystal

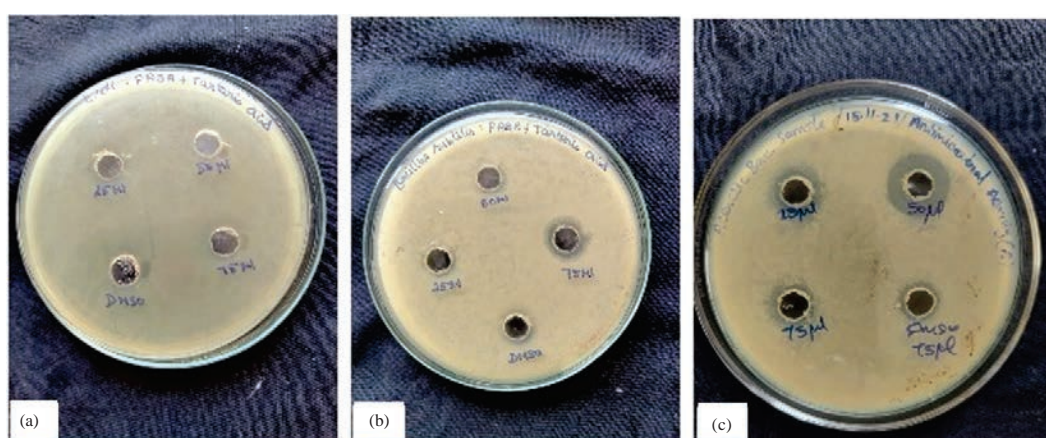
Fig. 11(a-b): Zone of inhibition of 4-carboxyanilinium tartrate crystal in, (a) *Escherichia coli* bacterial strains, (b) *Bacillus subtilis* bacterial strains and (c) *Acinetobacter baumannii* bacterial strains

Table 4: Diameter of zones of inhibition (mm) of 4-carboxyanilinium tartrate crystal against microorganisms

Bacteria	Plant concentration ($\mu\text{g mL}^{-1}$)		
	25	50	75
<i>Escherichia coli</i>	NZ	NZ	NZ
<i>Bacillus subtilis</i>	6 mm	8 mm	9 mm
<i>Acinetobacter baumannii</i>	7 mm	9 mm	7 mm

*NZ: No zone of inhibition

Antibacterial analysis: The 4-carboxyanilinium tartrate crystal sample was tested for antibacterial activity against *Escherichia coli*, *Bacillus subtilis* and *Acinetobacter baumannii* bacterial strains by agar well diffusion method with different concentrations of 25, 50 and 75 μL . Plant extracts of 50 mg mL^{-1} concentration were prepared in Dimethyl Sulfoxide (DMSO) as a positive control. The plates are incubated at the temperature of 37°C for 18-24 hrs. The progress of the inhibition zone in the well was measured and noted. The antibacterial behaviour of three different bacterial strains is shown in Fig. 11a-c and the results are reported in Table 4. According to the zone of inhibition, *Bacillus subtilis* and *Acinetobacter baumannii* exhibit the highest sensitivity towards 4-carboxyanilinium tartrate crystal while, *Escherichia coli* shows no sensitivity among the tested microorganisms.

CONCLUSION

The single crystal of 4-carboxyanilinium tartrate was grown by slow evaporation technique in an aqueous ethanol solution at room temperature. Crystal structure and lattice parameters were determined using

single crystal X-ray diffraction and it showed the monoclinic system which was found in close covenant with the earlier report's experimental findings. The good crystalline nature of grown crystals was confirmed by the powder XRD study. The average particle size was determined as 55 nm and the diffraction peaks were indexed using INDX software. The presence of various functional groups was confirmed by FT-IR and FT-Raman spectroscopy. The optical band gap was calculated from absorbance data using Tauc relation and found to be 3.75 eV. The surface morphology and elemental composition were determined by SEM/EDX studies, which showed that the grown crystal was of good quality. The antibacterial activity was performed against three kinds of bacterial strains by the agar well diffusion method for various concentrations. *Bacillus subtilis* and *Acinetobacter baumannii* exhibited the highest sensitivity towards the grown crystal while, *Escherichia coli* showed no warmth among the tested microbes.

SIGNIFICANCE STATEMENT

This study discovered the drug complex crystal with the organic acid combination that can be beneficial for the biological and pharmacological field. This study will help the researchers to uncover the critical areas of complex crystal synthesis that many researchers were not able to explore. Thus a new theory on the formation of drug complex crystal with organic acid combination may be arrived at.

REFERENCES

1. Song, G.C., H.K. Choi and C.M. Ryu, 2013. The folate precursor *para*-aminobenzoic acid elicits induced resistance against *Cucumber mosaic virus* and *Xanthomonas axonopodis*. *Ann. Bot.*, 111: 925-934.
2. Muthuselvi, C., M. Pandeewari and S.S. Pandiarajan, 2017. Spectral and antimicrobial activity studies on 4-carboxyanilinium nitrate crystal. *Asian J. Appl. Sci.*, 10: 170-178.
3. Akberova, S.I., 2002. New biological properties of *p*-aminobenzoic acid. *Biol. Bull. Russ. Acad. Sci.*, 29: 390-393.
4. Patel, H.M., V. Bhardwaj, P. Sharma, M.N. Noolvi, S. Lohan, S. Bansal and A. Sharma, 2019. Quinoxaline-PABA bipartite hybrid derivatization approach: Design and search for antimicrobial agents. *J. Mol. Struct.*, 1184: 562-568.
5. Crisan, M.E., P. Bourosh, M.E. Maffei, A. Forni, S. Pieraccini, M. Sironi and Y.M. Chumakov, 2014. Synthesis, crystal structure and biological activity of 2-hydroxyethylammonium salt of *p*-aminobenzoic acid. *PLoS ONE*, Vol. 9. 10.1371/journal.pone.0101892.
6. Zhou, L., Y. Ji, C. Zeng, Y. Zhang, Z. Wang and Xi Yang, 2013. Aquatic photodegradation of sunscreen agent *p*-aminobenzoic acid in the presence of dissolved organic matter. *Water Res.*, 47: 153-162.
7. Drozd, K.V., S.G. Arkhipov, E.V. Boldyreva and G.L. Perlovich, 2018. Crystal structure of a 1:1 salt of 4-aminobenzoic acid (vitamin B₁₀) with pyrazinoic acid. *Acta Crystallogr. Sect. E: Crystallogr. Commun.*, E74: 1923-1927.
8. Vasilieva, S., 2001. *Para*-aminobenzoic acid inhibits a set of SOS functions in *Escherichia coli* K12. *Mutat. Res. Genet. Toxicol. Environ. Mutagen.*, 496: 89-95.
9. Athimoolam, S. and S. Natarajan, 2006. Hydrogen-bonding motifs in 4-carboxyphenylammonium nitrate and perchlorate monohydrate and in bis(4-carboxyphenylammonium) sulfate. *Acta Crystallogr., Sect. C: Struct. Chem.*, C62: o612-o617.
10. Hu, Z., J. Liu, L. Shen, D. Xu and Y. Xu, 2002. Separation of 4-aminobenzoic acid by cocrystallization: Crystal structure of the complex of 4-aminobenzoic acid with (2*R*,3*R*)-tartaric acid. *J. Chem. Crystallogr.*, 32: 525-529.
11. Han, L.J., S.P. Yang, X. Tao and Y.F. Ma, 2011. 4-carboxyanilinium chloride. *Acta Crystallogr. Sect. E: Crystallogr. Commun.*, Vol. E67. 10.1107/S1600536811046721.
12. Wiklund, P. and J. Bergman, 2006. The chemistry of anthranilic acid. *Curr. Org. Synth.*, 3: 379-402.
13. Benali-Cherif, N., A. Direm, F. Allouche and K. Soudani, 2007. 4-Carboxyanilinium hydrogensulfate. *Acta Crystallogr. Sect. E: Crystallogr. Commun.*, E63: o2054-o2056.
14. Benali-Cherif, N., A. Direm, F. Allouche and K. Soudani, 2007. Hydrogen bonding in 4-carboxyanilinium dihydrogenphosphate. *Acta Crystallogr. Sect. E: Crystallogr. Commun.*, E63: o2272-o2274.

15. Muthuselvi, C., A.S. Princy and S.S. Pandiarajan, 2017. Growth and characterization of 4-carboxyanilinium dihydrogen phosphate semi-organic complex crystal. *Asian J. Appl. Sci.*, 10: 159-169.
16. Athimoolam, S. and S. Natarajan, 2007. 4-Carboxyanilinium (2*R*,3*R*)-tartrate and a redetermination of the α -polymorph of 4-aminobenzoic acid. *Acta Crystallogr. Sect. C: Struct. Chem.*, C63: o514-o517.
17. Subramanian, N., N. Sundaraganesan, S. Sudha, V. Aroulmoji, G.D. Sockalingam and M. Bergamin, 2011. Experimental and theoretical investigation of the molecular and electronic structure of anticancer drug camptothecin. *Spectrochim. Acta Part A: Mol. Biomol. Spectrosc.*, 78: 1058-1067.
18. Ahamed, S.R., J. Balaji and P. Srinivasan, 2018. Growth and characterization of organometallic NLO material: Cesium hcontri hydrogen tartrate. *Mater. Res. Innovations*, 22: 294-301.
19. Nagalakshmi, R., V. Krishnakumar, H. Hagemann and S. Muthunatesan, 2011. Polarized raman and hyperpolarizability studies of hydroxyethylammonium (L) tartrate monohydrate for quadratic nonlinear optics. *J. Mol. Struct.*, 988: 17-23.
20. Marchewka, M.K., S. Debrus, A. Pietraszko, A.J. Barnes and H. Ratajczak, 2003. Crystal structure, vibrational spectra and nonlinear optical properties of L-histidinium-L-tartrate hemihydrate. *J. Mol. Struct.*, 656: 265-273.
21. Muthuselvi, C., I. Ilakkiya, I. Parameswar and A. Alagumari, 2021. Gel growth and characterization of sodium hydrogen tartrate monohydrate organo-metallic single crystal. *Curr. Res. Chem.*, 13: 7-14.
22. Sun, J., L. Yao, Z. Gao, S. Peng, C. Wang and Y. Qiu, 2010. Surface modification of PET films by atmospheric pressure plasma-induced acrylic acid inverse emulsion graft polymerization. *Surf. Coat. Technol.*, 204: 4101-4106.